© 2016. Published by The Company of Biologists Ltd | Development (2016) 143, 2842-2852 doi:10.1242/dev.133173

RESEARCH ARTICLE

Quadruple zebrafish mutant reveals different roles of Mesp genes in somite segmentation between mouse and zebrafish

Taijiro Yabe[1,2], Kazuyuki Hoshijima[3], Takashi Yamamoto[4] and Shinji Takada[1,2,*]

ABSTRACT

The segmental pattern of somites is generated by sequential conversion of the temporal periodicity provided by the molecular clock. Whereas the basic structure of this clock is conserved among different species, diversity also exists, especially in terms of the molecular network. The temporal periodicity is subsequently converted into the spatial pattern of somites, and *Mesp2* plays crucial roles in this conversion in the mouse. However, it remains unclear whether Mesp genes play similar roles in other vertebrates. In this study, we generated zebrafish mutants lacking all four zebrafish Mesp genes by using TALEN-mediated genome editing. Contrary to the situation in the mouse *Mesp2* mutant, in the zebrafish Mesp quadruple mutant embryos the positions of somite boundaries were clearly determined and morphological boundaries were formed, although their formation was not completely normal. However, each somite was caudalized in a similar manner to the mouse *Mesp2* mutant, and the superficial horizontal myoseptum and lateral line primordia were not properly formed in the quadruple mutants. These results clarify the conserved and species-specific roles of Mesp in the link between the molecular clock and somite morphogenesis.

KEY WORDS: Somitogenesis, Segmentation, Boundary formation, Mesp, Zebrafish, TALEN

INTRODUCTION

Basic body structures are highly conserved among vertebrates. It is still not clear, however, to what extent the molecular mechanism underlying the generation of such structures is conserved. Somites, which are basic structures giving rise to skeletal muscle, vertebrae and dermis, are periodically generated in an anterior-to-posterior fashion during early embryogenesis. The periodical generation of somites can be generally explained by the 'clock and wavefront model', in which the timing and position of somite boundary formation are determined based on the spatiotemporal information generated by periodical activation of the 'segmentation clock' and posterior regression of the 'determination front', respectively (Cooke and Zeeman, 1976). Integration of such temporal and spatial information achieves the cyclic generation of presumptive somites in the anterior presomitic mesoderm (PSM). This model is supported by intensive studies using a number of different model animals to identify genes involved in the segmentation of somites (Hubaud and Pourquié, 2014; Oates et al., 2012).

However, in contrast to this conserved scheme of segmentation, the molecular network involved in the generation and propagation of the segmentation clock may not necessarily be conserved (Krol et al., 2011). In the mouse, distinct but mutually related molecular clocks have been identified, including the oscillatory activation of the transcriptional repressor Hes7, and Notch, Fgf and Wnt signaling, whose oscillations are generated by negative-feedback regulation (Hubaud and Pourquié, 2014). Her family genes, which are homologs of mouse Hes genes, have been considered as the core of the clock in the zebrafish. Oscillation of these genes is generated and maintained by self-repression and association with other Her proteins (Hubaud and Pourquié, 2014; Oates et al., 2012; Schröter et al., 2012; Trofka et al., 2012).

To understand the biological significance of the diversity of the molecular clock among species, it is important to show how such diversity is reflected in the morphogenesis of somites. Once the molecular clock is established, this temporal periodicity is converted into the spatial pattern of somites at or around the wave front. This conversion process consists of three steps (Dahmann et al., 2011; Saga, 2012a; Zhao et al., 2015). First, the position of a presumptive somite boundary is determined in the anterior PSM (boundary positioning). Next, epithelialization of cells adjacent to the presumptive boundary occurs to generate the physical segmental boundary of the somite (physical boundary formation). In parallel to physical boundary formation, rostro-caudal (R-C) polarity is established within the somite to provide positional information by which various type cells are generated from the somite in later development (R-C polarity formation).

In mouse somitogenesis, Mesp2, a basic helix-loop-helix (bHLH) transcriptional factor, functions as the key regulator in all three steps of this conversion process (Saga, 2012a). Mesp2 activates the expression of *Ripply1* and *Ripply2*, which determine the somite boundary position through repression of Tbx6 protein (Oginuma et al., 2008; Takahashi et al., 2010; Zhao et al., 2015). *Mesp2* expression is then restricted to the rostral half of predicted somite and activates the expression of *Epha4*, which is proposed to be involved in morphogenesis of the physical segmental boundary (Nakajima et al., 2006). In addition, Mesp2-dependent inhibition of Notch signaling, which is essential to induce the caudal identity of somite, is required for the establishment of the rostral identity of a somite (Takahashi et al., 2000; Morimoto et al., 2005; Sasaki et al., 2011). Since *Mesp2* expression, which is periodical in the anterior PSM, is directly induced by periodically activated Notch signaling in mouse somitogenesis, Mesp2 is the master regulator connecting the segmentation clock to somite morphogenesis in the mouse (Morimoto et al., 2005; Yasuhiko et al., 2006). However, because of the lack of comparative analysis of the role of Mesp in other vertebrates, it is still uncertain as to what extent the molecular

[1]Division of Molecular and Developmental Biology, Okazaki Institute for Integrative Bioscience and National Institute for Basic Biology, National Institutes of Natural Sciences, Okazaki, Aichi 444-8787, Japan. [2]Department for Basic Biology, SOKENDAI (The Graduate University for Advanced Studies), Okazaki, Aichi 444-8787, Japan. [3]Department of Human Genetics, University of Utah, Salt Lake City, UT 84112, USA. [4]Department of Mathematical and Life Sciences, Graduate School of Science, Hiroshima University, Hiroshima 739-8526, Japan.

*Author for correspondence (stakada@nibb.ac.jp)

S.T., 0000-0003-4125-6056

Received 25 November 2015; Accepted 17 June 2016

Development (2016) 143, 2842-2852 doi:10.1242/dev.133173

mechanism of this connection is conserved in other animals in which the temporal periodicity is established by a different molecular mechanism to that in the mouse.

Like the mouse, the zebrafish is a typical model animal widely used for genetic studies. The zebrafish has four Mesp genes, *mespaa*, *mespab*, *mespba* and *mespbb*, all of which are expressed in the anterior PSM during somitogenesis (Sawada et al., 2000; Durbin et al., 2000; Cutty et al., 2012). However, the roles of these Mesp genes in somitogenesis remain unclear. Zebrafish embryos injected with Mesp mRNA are defective in somite boundary and R-C polarity formation in their somites (Sawada et al., 2000; Durbin et al., 2000). In contrast, the injection of antisense morpholino specific for *mespba* and *mepbb* causes abnormal myogenesis but no obvious defect in the somite boundary formation (Windner et al., 2015). Thus, to clarify genetically whether these Mesp genes play a role in somitogenesis, we sought to generate a quadruple mutant for all of the zebrafish Mesp genes by using the TALEN-mediated genome editing approach. Analysis of the quadruple mutant embryos highlighted the conserved roles of Mesp genes between different species and also the species-specific mechanism governing positioning of the somite boundary.

RESULTS

Generation of Mesp quadruple mutants in zebrafish

It was predicted that the Mesp gene mutations would be null because mutant fish lines used in this study carried frame-shift mutations upstream of the bHLH domain of each Mesp gene (see also Discussion). Homozygous mutant embryos for any of the four Mesp genes, however, showed no obvious defect during embryogenesis, suggesting that the four genes are functionally redundant. Then, we sought to generate quadruple homozygotes for these four Mesp genes. Since *mespaa* and *mespba*, as well as *mesppab* and *mespbb*, are located close to each other on the same chromosome, the recombination rate between each pair of these genes would be predicted to be quite low (Fig. 1A). Thus, we first generated two independent double heterozygotes by introducing a *mespaa* mutation into *mespba*/+ fish and *mespab* mutation into *mespbb*/+ fish. The double mutants appeared normal (Fig. 2C-E). By sequential intercrossing between these double mutant lines, we finally obtained the *mespaa*^{kt1017}; *mespba*^{kt1004}; *mespab*^{kt1002}; *mespbb*^{kt1009} quadruple homozygous mutant, referred to as the Mesp quadruple mutant, which lacked the function of all Mesp genes (Fig. 1B).

In contrast to mouse embryos defective in either or both *Mesp1* and *Mesp2*, which show several obvious defects during early embryogenesis (Saga et al., 1997; Saga et al., 1999; Kitajima et al., 2000), the phenotype of zebrafish Mesp quadruple mutants appeared milder. In contrast to the mouse *Mesp2* mutant, in which all somite boundaries are disrupted, most of somite boundaries, except the most anterior 3-5 somites, were still generated in the Mesp quadruple mutant embryos (Fig. 2A,B,C,F); although the morphology of each somite appeared to be different from the normal, chevron-shaped, one (Fig. 2C′,F). Furthermore, the defective mesoderm formation seen in the mouse *Mesp1*/*Mesp2* double-mutant embryo and abnormal heart development reported in the mouse *Mesp1* mutant were not observed in the Mesp quadruple mutant embryos (Fig. S1). We also noted that development of the lateral plate mesoderm, which had been reported to be impaired in *mespaa* morphants (Hart et al., 2007), was normal in Mesp quadruple mutant embryos (Fig. S1).

Several possibilities exist to explain this inconsistency between mutant and morphant phenotypes. One is that the TALEN-mediated mutations might not be null. However, in all of the mutations generated in this study, we introduced frame-shift mutations upstream of the bHLH domain, which is essential for the DNA binding of the Mesp protein. We also confirmed by PCR that unpredicted splicing (Fig. S2A), like exon skip, did not occur in the mutant embryos. Another possibility is that a small peptide

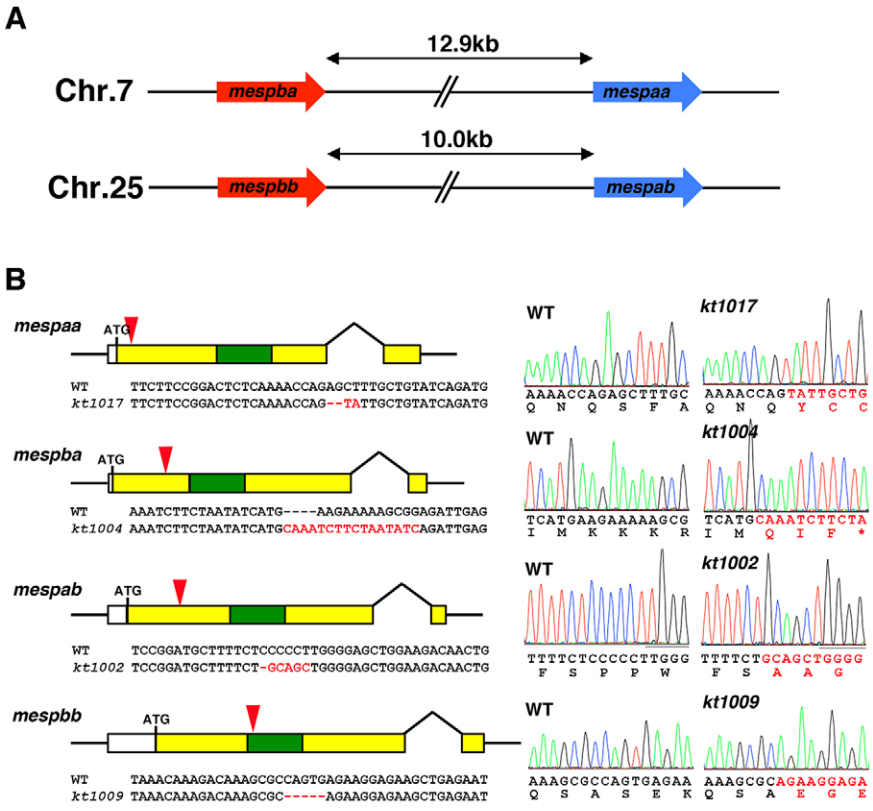

Fig. 1. Generation of Mesp gene mutants using TALEN. (A) Location of the four Mesp genes in the zebrafish genome. *mespaa* and *mespb* are tightly linked to *mespba* and *mespbb*, respectively. (B) Schema showing the mutations in the four Mesp genes. The structure of the genes is shown on the left. Collared boxes indicate coding regions; and green boxes, the regions encoding the bHLH domain. Red arrowheads indicate the approximate position of each mutation. The sequences around the mutation are given below the schema of the gene structure. Red characters indicate the mutated sequence. The right panel shows the sequence chart obtained by the direct sequencing of PCR products amplified from the cDNA obtained from wild-type and Mesp quadruple homozygous mutant embryos.

Development (2016) 143, 2842-2852 doi:10.1242/dev.133173

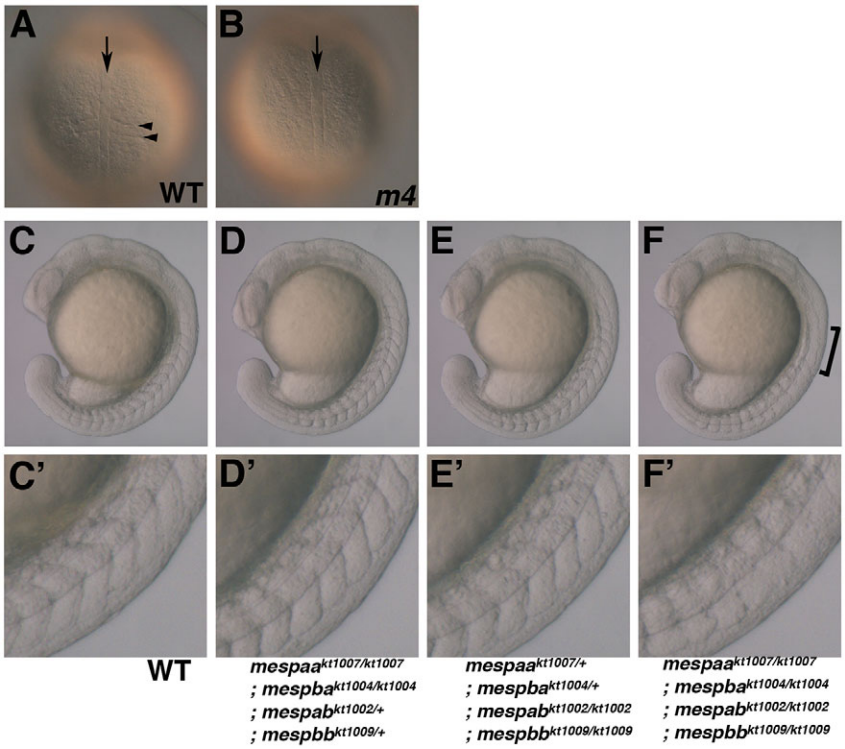

Fig. 2. Phenotype of the Mesp quadruple homozygous mutant. (A,B) Dorsal view of wild type and Mesp quadruple homozygous mutant at the 1-somite stage. The arrowhead points to the morphological somite boundary. The arrows indicate the notochord. (C-F) Morphology of wild-type (C), *mespaa* and *mespba* double mutant (D), *mespab* and *mespbb* double mutant (E), and Mesp quadruple homozygous mutant (*m4*; F) embryos at the 18-somite stage. Magnified images are also indicated (C′-F′). The bracket indicates the impaired somite boundary in the Mesp quadruple mutant.

fragment containing the bHLH domain, which may be alternatively translated from an AUG site downstream from the first AUG site, might have had an effect on the phenotype. Sequencing analysis revealed that such a possibility could not be excluded in the case of *mespab* and *mespbb* alleles. Thus, we further generated additional mutant alleles for these two Mesp genes, from which a functional product theoretically cannot be generated. However, the quadruple mutants containing these two alleles did not exhibit any additional defect (Fig. S2B-N). These findings strongly suggest that the TALEN-mediated mutations generated in this study were null.

Furthermore, we examined the possible contribution of maternally deposited Mesp gene transcripts or proteins to the phenotype of the Mesp quadruple mutant by generating maternal and zygotic (MZ) Mesp quadruple mutants. We did so by crossing Mesp quadruple homozygous fish, which could survive to adulthood and were fertile, because RT-PCR analysis revealed that maternally supplied transcripts of *mespaa* and *mespba* were detectable in zebrafish embryos. MZ-Mesp quadruple mutants, however, did not show enhanced abnormality in early mesoderm formation and patterning. Taken together, the lack of several phenotypes observed in mouse Mesp mutants and the zebrafish Mesp morphant was not caused by inefficient disruption of gene function in the quadruple mutant. Thus, the Mesp function was less critical during early embryogenesis in the zebrafish compared with that in the mouse or its function might have been compensated by functionally related genes. For instance, since a T-box protein, encoded by *tbx16* (previously known as *spadetail*) and a homeobox protein, encoded by *mixl1* (*bonny and clyde*), are redundantly required for cardiac mesoderm specification during zebrafish embryogenesis (Griffin and Kimelman, 2002), the lack of Mesp function might have also been compensated by these transcriptional factors in the Mesp quadruple mutant. As the MZ-Mesp quadruple mutant seemed to be identical to the zygotic mutant, we used the former embryos for subsequent experiments.

Positioning of somite boundaries is mostly unaffected in Mesp quadruple mutants

To better understand the role of Mesp genes in zebrafish somitogenesis, we then precisely examined somite development in the Mesp quadruple mutant embryos. As shown above, the homozygous Mesp quadruple mutant lacked several boundaries between its anterior somites. Only the Mesp quadruple mutant embryo showed this defect among the siblings obtained by the crossing of Mesp quadruple heterozygous parents, indicating highly redundant functions of Mesp genes. A similar defect specific to anterior somites is observed in *fn1* or *itga5* mutants, in which anterior somite boundaries are initially formed but not maintained (Koshida et al., 2005; Jülich et al., 2005). By contrast, the anterior boundaries were not generated at all in the Mesp quadruple mutant, indicating that Mesp function is not closely correlated with that of *fn1* and *itga5* (Fig. 2A,B).

In contrast to a few anterior somites, somite boundaries were created between most of the posterior somites. Previous studies revealed that the somite boundary could be established through two distinct processes: positioning of the somite boundary and morphogenesis of the actual physical boundary. The position of presumptive boundaries is initially defined at the anterior edge of the Tbx6 protein domain in both the mouse and zebrafish (Oginuma et al., 2008; Wanglar et al., 2014). In mouse *Mesp2* mutant embryos, this anterior edge is not properly created; rather the Tbx6 protein domain is anteriorly extended. In the zebrafish Mesp quadruple mutant embryos, however, the anterior edge of the Tbx6 protein domain was still clearly formed as observed in wild-type embryos (Fig. 3A,B,D,E). However, *ripply1* and *ripply2* double-homozygous embryos, which we also generated by TALEN-mediated mutagenesis, exhibited abnormal extension of the Tbx6 protein domain, indicating that the function of Ripply genes is essential for the positioning of somites, as predicted by the results of morpholino-based studies (Fig. 3C,F and Fig. S3). Thus, the

Development (2016) 143, 2842-2852 doi:10.1242/dev.133173

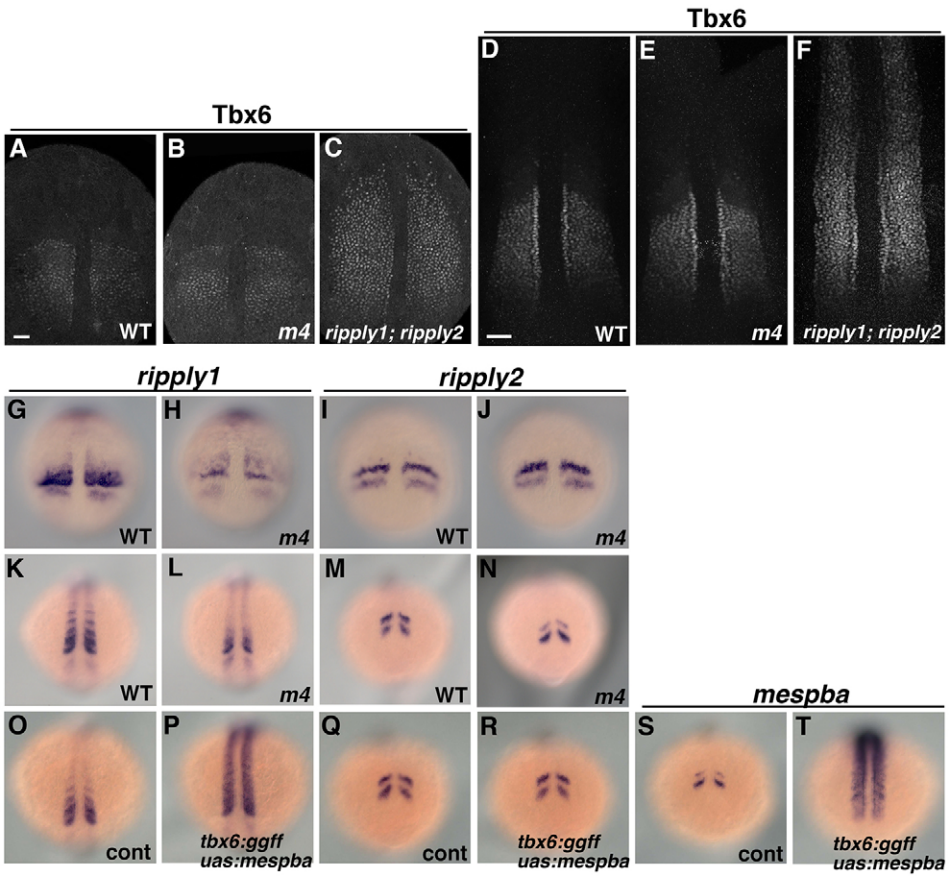

Fig. 3. Somite positioning in the Mesp quadruple mutant. (A-F) Immunostaining of Tbx6 in wild-type, Mesp quadruple mutant and *ripply1; ripply2* double mutant embryos fixed at the 1-somite stage (A-C) and 9-somite stage (D-F). In wild-type and Mesp quadruple mutant embryos, a clear anterior border of the Tbx6 protein domain is seen. In contrast, in the *ripply1; ripply2* double mutant embryo, this domain has expanded anteriorly. (G-N) Expression of *ripply1* (G,H,K,L) and *ripply2* (I,J,M,N) in wild-type (G,K,I,M) and Mesp quadruple mutant (H,L,J,N) embryos. In the Mesp quadruple mutant, the expression of *ripply1* in the anterior PSM is not affected, although expression in the somite region is severely reduced at the 1-somite stage (G,H; 100%; *n*=15) and 11-somite stage (K,L; 100%; *n*=14). Expression of *ripply2* is not affected at the 1-somite stage (I,J; 100%; *n*=17) or 11-somite stage (M,N; 100%; *n*=15). (O-T) The effect of overexpression of *mespba* on the expression of *ripply1* and *ripply2* in embryos fixed at the 11-somite stage. In *tbx6: ggff; uas:mespba* double transgenic fish, the ectopic expression of *mespba* is detected in the mature somite region and anterior PSM (S,T; *n*=10; 100%). The expression of *ripply1* at the anterior PSM is not affected by the overexpression of *mespba*, although the expression of somite region is strongly enhanced (O,P; 100%; *n*=11). The expression of *ripply2* is not altered by the overexpression of *mespba* (Q,R,G,H; 100%; *n*=7). Scale bars: 50 µm.

position of the segmental boundary was determined by a Mesp-independent but Ripply-dependent manner in zebrafish.

Since Mesp2 regulates the expression of *Ripply1* and *Ripply2*, which subsequently define the anterior edge of the Tbx6 protein domain, in mouse somitogenesis (Takahashi et al., 2010; Morimoto et al., 2007), we next examined the role of Mesp for Ripply gene expression in zebrafish. In the wild-type embryo, *ripply1* was expressed at both the anterior PSM and rostral compartment of each somite; whereas *ripply2* was expressed in two to three strips in the anterior PSM (Fig. 3G,I,K,M). In the Mesp quadruple mutant, although the striped expression pattern of *ripply1* was severely perturbed in somites, *ripply1* and *ripply2* expression patterns were not affected in the anterior PSM compared with that in the siblings (Fig. 3H,J,L,N). By contrast, when *mespba* was overexpressed in somites and in the anterior PSM region by using the *tbx6; gfp-gal4* (*ggff*) driver (Fig. S4), expression of *ripply1* and *ripply2* was not ectopically induced in the anterior PSM; although somite expression of *ripply1* was expanded to the caudal compartment of somites (Fig. 3O-T). Thus, in contrast to mouse, zebrafish *ripply1* and *ripply2* were expressed in the anterior PSM independent of Mesp function. The unaffected expression of *ripply1* and *ripply2* in the anterior PSM appears to preserve the normal positioning of somite boundaries in the Mesp quadruple mutant.

Morphogenesis of physical somite boundaries is partly disrupted in Mesp quadruple mutants

Next, we examined whether zebrafish Mesp genes were involved in morphogenesis of the physical boundary. In our preliminary observation of the Mesp quadruple mutant fish under a stereomicroscope, almost all of the somite boundaries, except for those of several anterior somites, were evident. However, more detailed analysis using Phalloidin staining revealed that the boundary morphology was partially disrupted, even in the posterior somites (Fig. 4A,B). During morphogenesis of somite boundaries in the zebrafish, initially established boundaries are gradually reinforced by the accumulation of ECM components such as fibronectin. This accumulation is required for the cells adjacent to the boundary to establish their apico-basal polarity, which is considered to be important for maintenance of the physical boundaries (Koshida et al., 2005). In the Mesp quadruple mutants, Fibronectin did accumulate at the somite boundaries; but the pattern of its assembly was partially disturbed (Fig. 4A,B). Thus, zebrafish Mesp plays a role in morphogenesis after the positioning of the presumptive boundaries; and its requirement is higher in the anterior somites than in the posterior ones.

Transplantation studies with zebrafish and chick embryos revealed that the repulsive interaction between Epha4 and EphrinB2 is sufficient to generate physical boundaries between transplants and host cells (Barrios et al., 2003; Watanabe et al., 2009). Considering the expression patterns of these genes, this repulsive interaction occurs prior to the accumulation of Fibronectin. Since *epha4* expression is directly regulated by Mesp2 during somitogenesis in the mouse, we next examined *epha4* expression in the Mesp quadruple mutant (Fig. 4C,D,G,H). In normal zebrafish embryos, *epha4* is expressed in a striped pattern in the anterior PSM and somites, and in a gradient fashion along the anterior-posterior (A-P) axis in the posterior PSM. In contrast, the striped expression pattern of *epha4* was completely absent in the Mesp quadruple mutant; however, the gradient in expression was not affected. Thus, Mesp was specifically required for the striped

Development (2016) 143, 2842-2852 doi:10.1242/dev.133173

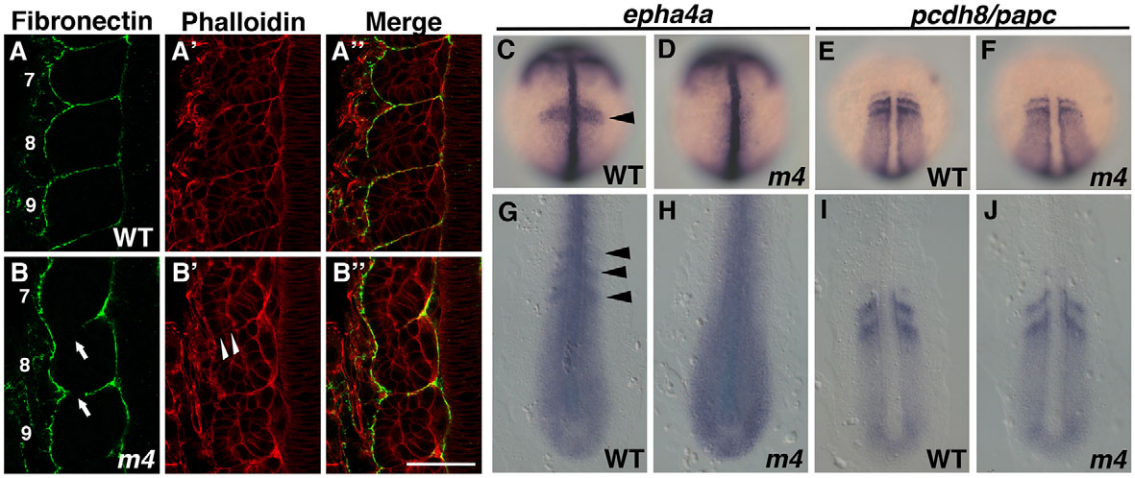

Fig. 4. Impaired formation of the morphological somite boundary in the Mesp quadruple mutant. (A,B) Wild-type (A-A″) and Mesp quadruple mutant (B-B″) embryos stained with anti-Fibronectin antibody (A,B) and Phalloidin (A′,B′). The numbers shown in A and B indicate the position of each somite from the most anterior one. White arrows indicate gaps of Fibronectin assembly at somite boundaries. White arrowheads indicate disruption of cell arrangement at a somite boundary. (C,D,G,H) Expression of *epha4a* in wild-type (C,G) and Mesp quadruple mutant (D,H) embryos. Embryos were fixed at the 1-somite stage (C,D) and the 8-somite stage (G,H). Striped expression of *epha4a* was lost in Mesp quadruple mutant embryos (D: 100%, *n*=9; H: 100%, *n*=12). Black arrowheads indicate striped expression of *epha4a* in the anterior PSM and somites. (E,F,I,J) Expression of *papc* in wild-type (E,I) and Mesp quadruple mutant (F,J) embryos. Embryos were fixed at the 1-somite stage (E,F) and the 11-somite stage (I,J). Striped expression of *papc* was not affected by disruption of the function of the four Mesp genes (F: 100%, *n*=9; J: 100%, *n*=18). Scale bar: 50 µm.

expression pattern of *epha4* in the zebrafish, as is reported to be the case in the mouse (Nakajima et al., 2006).

On the other hand, previous studies suggested that *pcdh8* (*papc*) is also involved in the morphogenesis of somite boundaries in the mouse (Rhee et al., 2003). In the wild-type embryo, striped expression of *pcdh8* was detected in the anterior PSM, whereas in the Mesp quadruple mutant, this striped expression pattern was not affected, although the expression level was slightly reduced, suggesting that the expression of *pcdh8* is mostly independent of Mesp (Fig. 4E,F,I,J). These results suggest that two parallel pathways – one Mesp dependent and one Mesp independent – regulate the morphogenesis of physical somite boundaries in the zebrafish.

Rostro-caudal polarity in somites is defective in Mesp quadruple mutant embryos

Mesp2 function is also essential for R-C polarity formation within a somite in the mouse. In zebrafish, although overexpression studies revealed that Mesp genes have a potential to induce rostral identity in somites, their physiological role in R-C polarity formation remains unclear (Sawada et al., 2000; Durbin et al., 2000). We found that expression of *tbx18* and *fgf8* in the rostral compartment of somites was completely missing in the Mesp quadruple mutant embryo (Fig. 5A-D,I,J). In contrast, the caudal expression of *uncx4.1* and *myod* expanded to the entire somite (Fig. 5E-H,K,L). We also confirmed that *mespba* was sufficient to induce *tbx18* expression and repress *uncx4.1* expression in the caudal half of each somite by overexpression of *mespba* in the anterior PSM and somite region by using *tbx6:ggff* driver (Fig. 5M-P). Thus, Mesp genes are necessary and sufficient to establish rostral identity in the zebrafish somite, as in mouse somitogenesis.

Previous studies reported that the R-C polarity in a somite is relayed to the sclerotome and essential for the pattern formation of vertebrae (Saga, 2012b). In the zebrafish Mesp quadruple mutant, duplication of hemal spines was observed in some vertebrae, implying that the spines of zebrafish vertebral bone were derived from the caudal compartment of somites, as in the case of the mouse vertebral arch, and duplicated by the caudalization of the somite (Fig. 5Q″,R″). In addition, the tips of several neural spines had split or fused abnormally (Fig. 5Q′,R′), suggesting that Mesp-dependent generation of the R-C polarity is required for the proper formation of vertebrae in later development. Although the R-C polarity was severely impaired along the entire body axis (Fig. 5B,F,J,L), skeletal defects were more evident in the anterior vertebrae than in the posterior ones. In contrast, the segmentation of vertebrae was not affected by Mesp mutation, supporting previous studies showing that vertebral columns are segmented independent of somite segmentation (Fleming et al., 2004).

Abnormalities in muscle development in Mesp quadruple mutant embryos

In the zebrafish Mesp quadruple mutant, none of the somites showed the chevron-shape morphology seen in the wild-type embryo (Fig. 2C,F). Such abnormal morphology is frequently caused by lack of the horizontal myoseptum, which is induced by hedgehog signaling and separates the dorsal and ventral compartment of fast muscle fibers (Halpern et al., 1993; Barresi et al., 2000). This horizontal myoseptum develops from adaxial cells, which are a subpopulation of paraxial mesoderm cells neighboring the notochord (Devoto et al., 1996). A population of these adaxial cells, located in the rostral part of a somite, differentiates into muscle pioneers (MPs), which are identified by their expression of *prox1* and *engrailed* (Felsenfeld et al., 1991; Roy et al., 2001). Then, these MPs elongate along the A-P axis and migrate laterally to generate the horizontal myoseptum, which is continuous with the slow muscle monolayer surrounding the lateral surface of the myotome, and divide the fast muscle myotome into its dorsal and ventral compartments.

In the Mesp quadruple mutant, differentiation into MPs, which were double positive for Prox1 and Engrailed, occurred normally, as observed in the wild-type embryo (Fig. 6A-C). However, in the Mesp quadruple mutant embryo, MPs remained close to the notochord, resulting in interruption of slow muscle fibers at the medial surface in the trunk (Fig. 6D,E). We also observed that

Development (2016) 143, 2842-2852 doi:10.1242/dev.133173

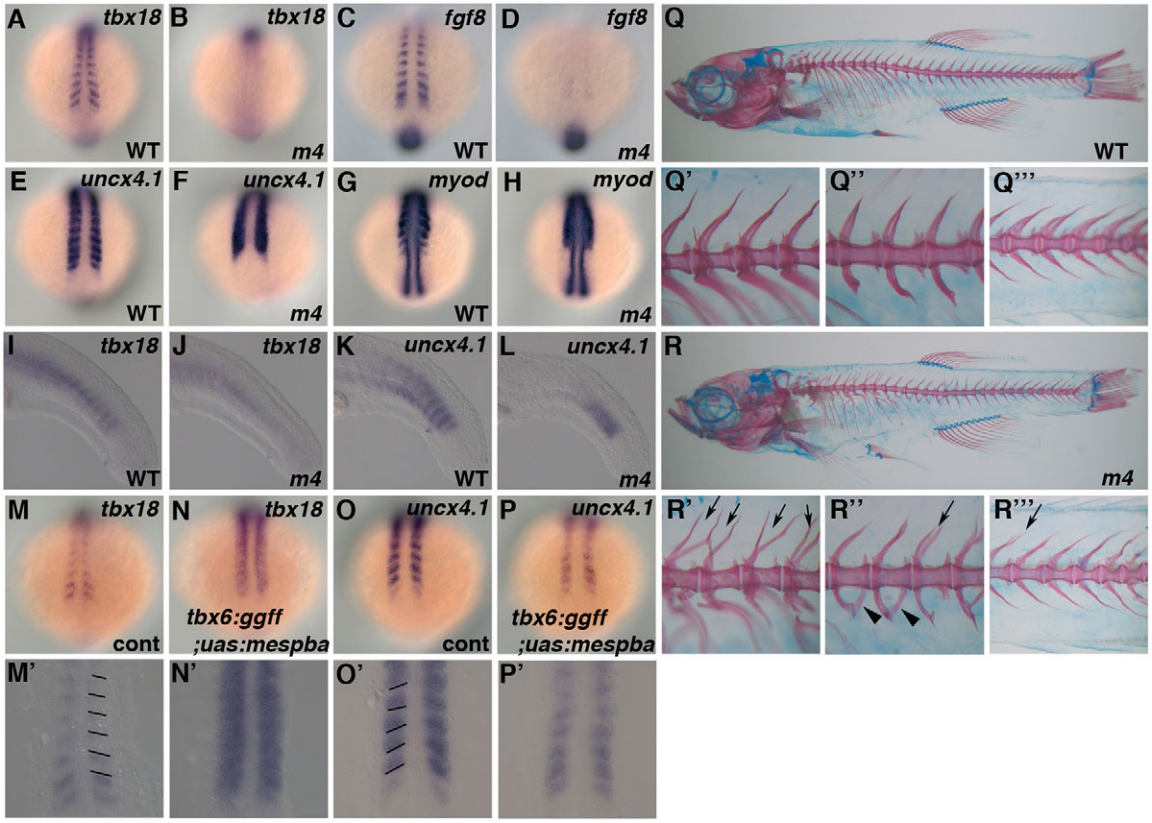

Fig. 5. Impaired rostro-caudal polarity in the Mesp quadruple mutant. Rostral expression of *tbx18* (A,B) and *fgf8* (C,D) is completely absent in the somites of Mesp quadruple mutant embryos at the 11-somite stage (100%, *n*=20 and 100%, *n*=13, respectively). In contrast, caudal expression of *uncx4.1* (E,F) and *myod* (G,H) has expanded in the entire somite of the Mesp quadruple mutant embryo at the same stage (100%, *n*=20 and 100%, *n*=18, respectively). The absence of *tbx18* expression (I,J) and expansion of *uncx4.1* expression (K,L) was also observed at the 28-somite stage (100%, *n*=15 and 100%, *n*=22, respectively). Expression of *tbx18* is increased (M,N) and that of *uncx4.1* is reduced (O,P) in the *tbx6:ggff; uas:mespba* double transgenic embryo at the 11-somite stage. Magnified images are also shown (M′-P′). The black lines indicate the position of somite boundaries. In the Mesp quadruple mutant at 30 dpf (R), hemal arches in several vertebral bones have been duplicated (arrowheads in R″) and neural arches are split (arrows in R′-R‴) compared with WT (Q). Magnified images are also indicated (Q′-Q‴,R′-R‴).

the expression of *cxcl12a* (*sdf1a*), a chemokine gene, at the superficial myoseptum had completely disappeared (Fig. 6F,G). These results indicated that Mesp function was essential for the correct distribution of MPs and their differentiation into a *cxcl12a*-positive superficial horizontal myoseptum.

In addition to the lack of the horizontal myoseptum, the number of myogenic progenitor cells that expressed *pax7* was decreased in the medial surface of somites and formation of fast muscle was abnormal in the quadruple mutant (Fig. 6H,I). These defects were similar to those shown by morpholino-mediated disruption of *mespba* and *mespbb* function (Windner et al., 2015). This complexity of defects in myotome development raised the question of which defect had the greatest contribution. To address this question, we performed a transplantation experiment in which the behavior of wild-type cells was monitored in a Mesp-deficient environment (Fig. 6J-L). In embryos whose phenotype was restored, as judged from *cxcl12a* expression in the medial surface of the trunk region, *cxcl12a* expression was restricted only in the wild-type donor cells, suggesting that the Mesp genes in adaxial cells, which are the progenitors of the *cxcl12a*-positive horizontal myoseptum, were required for proper formation of the horizontal myoseptum.

Expression of *cxcl12a* in the superficial horizontal myoseptum was reported to have important roles in the pattern formation of various tissues and cells in the body surface, including migration of the posterior lateral line (pLL) primordium and distribution of pigment cells at the body surface (David et al., 2002; Svetic et al., 2007). In the wild-type embryo, neuromasts, which are repetitively deposited from the pLL primordium during its migration, were aligned along the A-P body axis in the trunk and tail (Fig. 7A). However, in the Mesp quadruple mutant embryo, few neuromasts were deposited in the anterior trunk region, suggesting that loss of *cxcl12a* expression in the medial surface of somites resulted in mis-migration of the pLL primordium (Fig. 7B). Disrupted expression of *cxcl12a* in the superficial horizontal myoseptum was reported to affect neural crest migration along the lateral pathway in *meox1* (*choker*) mutants, resulting in a disturbed pattern of pigment cells (Svetic et al., 2007). Thus, expression of this chemokine ligand in the medial surface of somites is required for proper alignment of pigment cells in medial body surface region. Similarly, the alignment of melanocytes and iridophores was severely disrupted in the Mesp quadruple mutant embryo (Fig. 7C-F). This phenotype suggests that formation of the superficial horizontal myoseptum, which is regulated by Mesp genes, is required for proper pigment pattern formation in later developmental stages.

DISCUSSION

In mouse somitogenesis, *Mesp2* functions as the master regulator to connect the spatiotemporal information, generated by the segmentation clock and determination wavefront, to the multiple

Development (2016) 143, 2842-2852 doi:10.1242/dev.133173

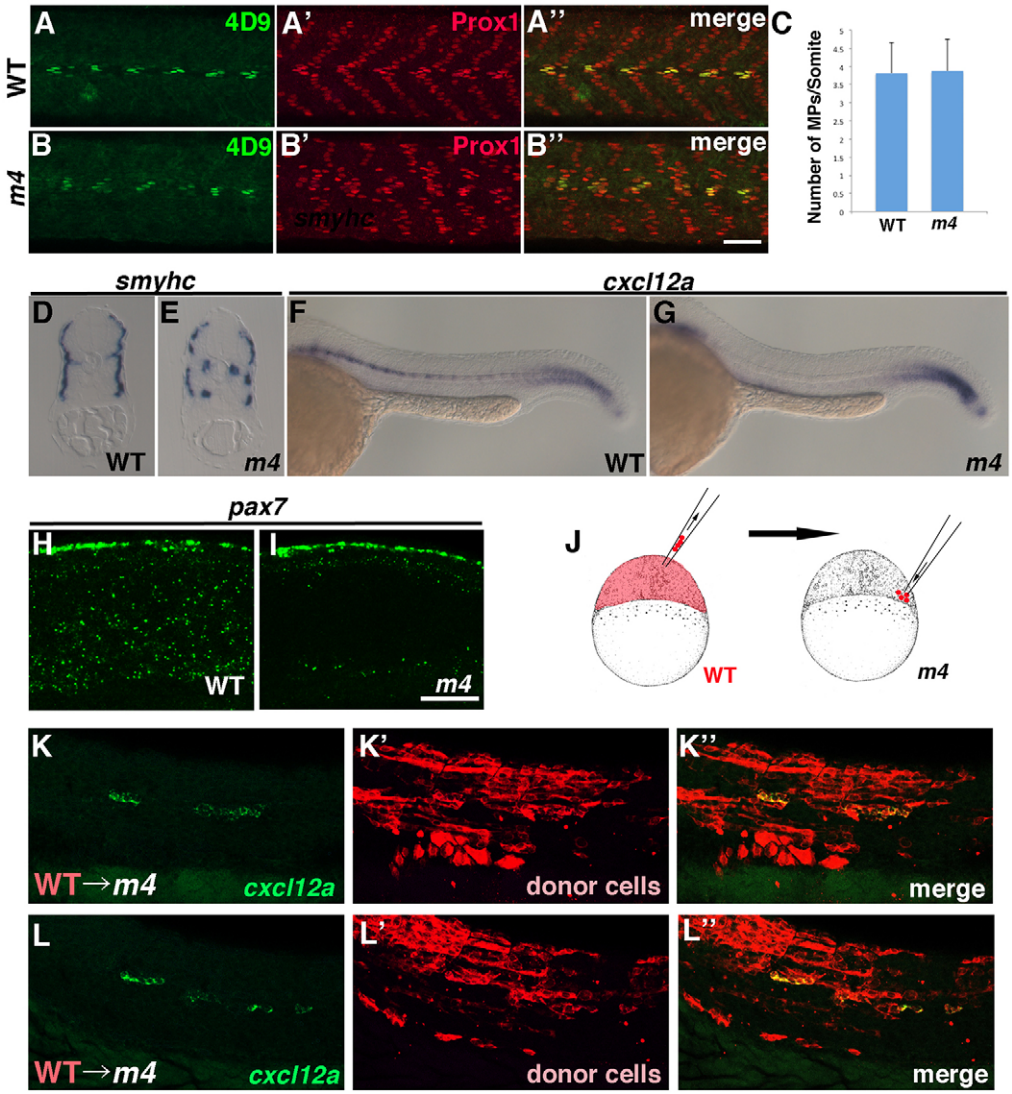

Fig. 6. Abnormal muscle development in the Mesp quadruple mutant. (A-C) Immunostaining of Engrailed (4D9) and Prox1 in the wild type (A) and Mesp quadruple mutant (B). Embryos were fixed at 24 hpf. Graph showing the numbers of MPs, identified as the 4D9 and Prox1 double-positive cells, in each somite in the wild-type and Mesp quadruple mutant embryos (C). The number of MPs at 24 hpf was counted in the 5-6 somites located in the most posterior part of the trunk region. A total of 16 somites were counted from 3 wild-type embryos and 23 somites from 4 mutant embryos. (D,E) Expression of *smyhc* in the wild-type and Mesp quadruple mutant embryos at 24 hpf. After whole-mount *in situ* hybridization, the embryos were transversely sectioned at the middle level of the yolk tube. (F,G) Expression of *cxcl12a* in the wild-type and Mesp quadruple mutant embryos at 24 hpf (100%, *n*=14). (H,I) Expression of *pax7* in wild-type and Mesp quadruple mutant embryos in the most posterior region of yolk tube. Embryos were fixed at the 20-somite stage. Scale bar: 50 µm. (J-L) Cell-autonomous function of Mesp in superficial horizontal myoseptum formation. (J) Schema for the transplantation experiment. The wild-type cells were transplanted at the marginal zone of Mesp quadruple mutant embryos at the blastula stage. Although the expression of *cxcl12a* is rescued in the transplanted embryo at 24 hpf (K,L), this expression is restricted to the donor cells (K″,L″). K and L show the rescued phenotype in different embryos. Although the rescued expression of *cxcl12a* was observed in a total of 42 cells in 10 embryos, this rescue occurred only in the donor cells in all cases.

processes of somite morphogenesis (Saga, 2012a). However, most of the functions of Mesp genes in zebrafish somitogenesis had remained unclear until now. In this study, we addressed this issue by generating Mesp mutants using TALEN-mediated mutagenesis. Although all Mesp single mutants showed no obvious defect throughout embryogenesis including somitogenesis, the Mesp quadruple mutant, which lacks the function of all four Mesp genes, exhibited defects in R-C polarity formation of its somites. The physical boundaries between somites were generated even in the Mesp quadruple mutant, although their formation was not completely normal, especially with respect to several anterior somites. In contrast, positioning of somite boundaries occurred normally even in the Mesp quadruple mutant. Thus, unlike in the mouse, zebrafish Mesp genes do not necessarily act as a master regulator to direct all of the three processes involved in somite morphogenesis; and the function of Mesp can be divided into conserved and species-specific functions.

Mesp in somite boundary positioning

The temporal periodicity generated by the segmentation clock is converted into a spatial pattern as the somite boundary to achieve the sequential and periodical generation of somites. Determination of the somite boundary position is the first step of this process. Previous studies revealed that the position of the somite boundary is defined as the anterior edge of the Tbx6 protein-expressing domain, which cyclically regresses posteriorly in a step-wise manner

Development (2016) 143, 2842-2852 doi:10.1242/dev.133173

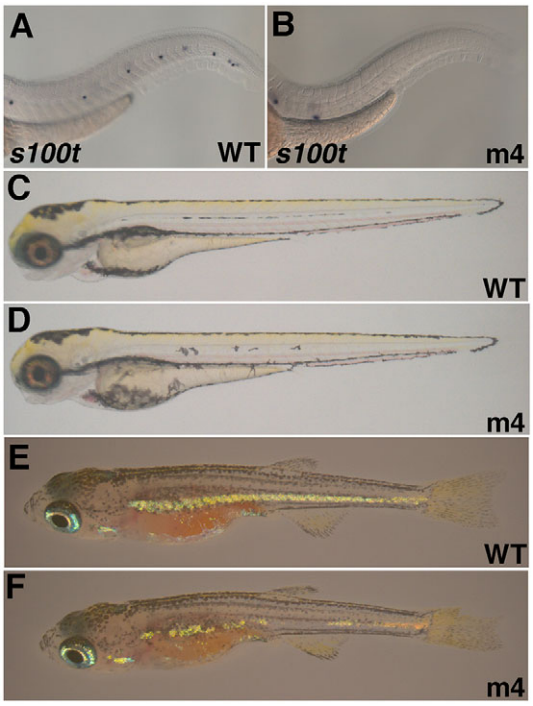

Fig. 7. Impaired patterning of medial body surface in the Mesp quadruple mutant. In wild-type embryos, the lateral line has been deposited at the medial surface of the trunk and tail region at 2 dpf (A). In contrast, the lateral line patterning is impaired in the Mesp quadruple mutant (B). In wild-type embryos, the melanocytes have elongated along the A-P axis and aligned themselves at the medial surface of the trunk and tail at 4 dpf (C). In contrast, in the Mesp quadruple mutant embryo, the melanocyte morphology and alignment have been disrupted (D). Unlike the case for the wild-type larva, in which the iridophores are aligned along the mediolateral body surface (E), a gap has formed in the aligned iridophores in the Mesp quadruple mutant at 30 dpf (F).

associated with the periodicity generated by the segmentation clock (Oginuma et al., 2008; Wanglar et al., 2014). In mouse somitogenesis, posterior regression of the Tbx6 domain is severely disrupted in the *Mesp2* mutant or *Ripply1* and *Ripply2* double-mutant embryos. A number of recent studies strongly suggest that *Mesp2*-dependent generation of anterior border of the Tbx6 protein domain is mediated by *Ripply1* and *Ripply2* in mouse somitogenesis (Takahashi et al., 2010; Zhao et al., 2015). For instance, expression of *Ripply1* and *Ripply2* is lost in *Mesp2*-deficient mouse embryos. Furthermore, the anterior border of the Tbx6 protein domain is properly established even in knock-in mice in which the *Mesp2* gene is completely replaced with *Ripply2* (Takahashi et al., 2010).

Although Ripply-dependent somite boundary positioning is conserved in zebrafish, the roles of Mesp in this process have remained unclear. Our genetic analysis revealed that Mesp genes but not Ripply genes, are dispensable for somite boundary positioning along the entire body axis in zebrafish. Moreover, we demonstrated that the effect of the Mesp mutation on *ripply1* expression is limited to the mature somite region and that the expression of *ripply1* and *ripply2* in the anterior PSM is regulated in a manner that is independent of the function of Mesp genes. Thus, the anterior border of the Tbx6 protein domain, which is consistent with the position of the presumptive somite boundary, is determined by *ripply1* and *ripply2* expression in the anterior PSM without the function of Mesp genes in the somites.

In contrast to most posterior somites, several anterior somites showed no clear boundaries in the Mesp quadruple mutant embryos. Of note, *ripply1* and *ripply2* expression in the anterior PSM and the formation of the anterior border of the Tbx6 protein domain were almost normal, even in the early somite stage. These results indicate that Mesp gene function is dispensable for the positioning of these anterior somites. Thus, the disrupted boundaries between several anterior somites observed in the Mesp quadruple mutant is not caused by impaired positioning of the somite boundaries.

Mesp in morphogenesis of physical boundaries

In somitogenesis, physical boundaries between somites are formed at the position defined by the anterior edge of the Tbx6 protein domain (Oginuma et al., 2008). The morphology of segmentation boundaries was partially disrupted in the Mesp quadruple mutant, even though the boundary positioning occurred normally. These results indicate that Mesp function is required for the proper formation of morphological boundaries in zebrafish. Consistent with this conclusion, recent analysis of mouse knock-in embryos in which the *Mesp2* gene was replaced with *Ripply2* showed that the function of Mesp2 is indispensable for generation of morphological boundaries (Zhao et al., 2015).

During morphogenesis of the segmentation boundaries, cells located at the somite boundary started to epithelialize after the initial establishment of the segment boundary. This initial boundary is considered to be generated by interaction between Eph and Ephrin, because transplantation studies using chick and zebrafish demonstrated that ectopic expression of *Epha4* is sufficient to generate segmental boundary-like structures in the unsegmented paraxial mesoderm (Barrios et al., 2003; Watanabe et al., 2009). Furthermore, the interaction between Epha4 and Ephrinb2a in zebrafish is sufficient for the initial generation of the segment boundary, but insufficient for the epithelialization, suggesting that additional molecular machinery is at work in the epithelialization (Barrios et al., 2003). Rather, the epithelialization further required the accumulation of the extracellular matrix component Fibronectin, mediated by Integrin alpha 5, which is activated by Epha4 (Jülich et al., 2015). In the Mesp quadruple mutant, the striped expression pattern of *epha4a* was lost, suggesting that aberrant boundary formation due to reduced expression of Epha4 causes a disruption in the accumulation of Fibronectin. However, the possibility that Mesp differentially regulates the boundary formation and epithelialization cannot be excluded.

In the Mesp quadruple mutant, the phenotype of somite boundary formation was mild in the posterior somites, suggesting involvement of a Mesp-independent molecular mechanism in this process. *pcdh8* is one of the candidate molecules involved in this Mesp-independent somite boundary formation, because its striped expression pattern at the anterior PSM was maintained in the Mesp quadruple mutant. At present, there is scant genetic evidence for the molecular mechanisms involved in cell border formation in vertebrate somitogenesis. Further studies using convenient reverse genetics approaches such as TALEN/CRISPR should clarify this issue.

Mesp genes in rostro-caudal polarity formation and muscle development

Previous studies with mice revealed that inhibition of Notch signaling by Mesp2, which is localized in the rostral compartment, is required for the establishment of the rostral identity within the somite (Morimoto et al., 2005; Saga, 2012a). Similar to the mouse, we demonstrated that Mesp function was essential and sufficient to

Development (2016) 143, 2842-2852 doi:10.1242/dev.133173

establish the rostral identity of somite even in the zebrafish. The molecular mechanism for the Mesp-dependent establishment of rostral identity remains unclear in zebrafish, because there is no genetic evidence supporting the involvement of Notch signaling in the establishment of the caudal identity, which is known to be the case in mouse somitogenesis.

Notably, the somite boundary, even though it was incomplete, was formed in the posterior body in the Mesp quadruple mutant, indicating that R-C polarity formation and somite boundary formation are distinguishable events in zebrafish. Similarly, a Mesp hypomorphic mouse embryo can form somite boundaries without clear R-C polarity, but the relationship between the two events is not completely identical to that in zebrafish (Nomura-Kitabayashi et al., 2002). In a hypomorphic mouse embryo, somite boundaries gradually disappear after their initial establishment, suggesting that proper R-C polarization is required for the maintenance of somite boundaries. In contrast, our study showed that morphological boundaries were maintained in zebrafish quadruple mutant embryos. Therefore, it seems plausible that not only establishment but also maintenance of somite boundary occur without R-C polarity in the zebrafish.

As previously shown by a knockdown study using morpholinos specific for *mespba* and *mespbb* (Windner et al., 2015), suppression of myogenic differentiation and induction of the dermomyotome in the rostral compartment of somites was defective in the Mesp quadruple mutant. In addition to the roles of Mesp genes in fast muscle fiber formation, our study also revealed essential roles of Mesp for the formation of the horizontal myoseptum, which consists of MPs, the progenitor cells of which are derived from the rostral compartment of adaxial cells (Nguyen-Chi et al., 2012). In the caudal compartment of adaxial cells, differentiation of MPs is repressed by Fgf signaling, which is specifically activated in the caudal compartment of somites. This process is possibly regulated by the R-C polarity in a manner that is independent of Mesp function, because the differentiation of MPs was not affected by the Mesp mutation. By contrast, the function of Mesp was essential for the lateral migration of MPs to generate the superficial horizontal myoseptum, which expresses *cxcl12a*. Thus, two different types of R-C polarity, Mesp independent and Mesp dependent, are likely to regulate specification and migration of MPs in the developing somite. The lateral migration of slow-twitch muscle was reported to be regulated by chemokine signaling and M- and N-cadherin (Chong et al., 2007; Cortés et al., 2003). A cell-autonomous function of Mesp possibly regulates the response to environmental cues provided by surrounding cells.

Differences in molecular mechanisms for somite formation in vertebrates

During vertebrate somitogenesis, the temporal information generated by the segmentation clock is converted to the spatial structure of the somites in the anterior PSM. Since in mouse somitogenesis, *Mesp2* expression is activated by the cooperative function of Tbx6 and Notch signaling, whose activity oscillates in the posterior PSM as the core component of the segmentation clock itself, *Mesp2* can be considered to act as the master key regulator to connect the segmentation clock to the spatial patterning and morphogenesis of somites (Yasuhiko et al., 2006; Saga, 2012a). However, in zebrafish, Özbuduk and Lewis previously reported that the Notch signaling is not essential for boundary formation of somites (Özbudak and Lewis, 2008). Thus, mouse and zebrafish appear to employ different molecular mechanism for this process, but the molecular mechanism to convert the segmentation clock to the somite boundary remains unclear in zebrafish.

In this study using the zebrafish, we demonstrated that the function of Mesp is not essential for Ripply-dependent boundary positioning, which is the earliest event to connect the segmentation clock to boundary formation (Fig. 8). This result indicates that, unlike in the mouse, neither Notch nor Mesp was essential for the clock-dependent positioning of the somite boundary in zebrafish. Thus, diversity of the molecular mechanism exists not only in terms of the segmentation clock but also with respect to the integration of the clock to the spatial structure in vertebrate somitogenesis. Our results suggest that the segmentation clock in the zebrafish regulates expression of *ripply1* and *ripply2* in a manner that is independent of Mesp function, although the molecular mechanism still remains unclear.

MATERIALS AND METHODS

Fish and embryos

Zebrafish with the TL2 background were used as the wild type, as described previously (Kishimoto et al., 2004). Collected embryos were grown at 28.5°C or 23.5°C and their developmental stages were determined according to morphological criteria (Kimmel et al., 1995). This study was performed in accordance with the Guidelines for Animal Experimentation

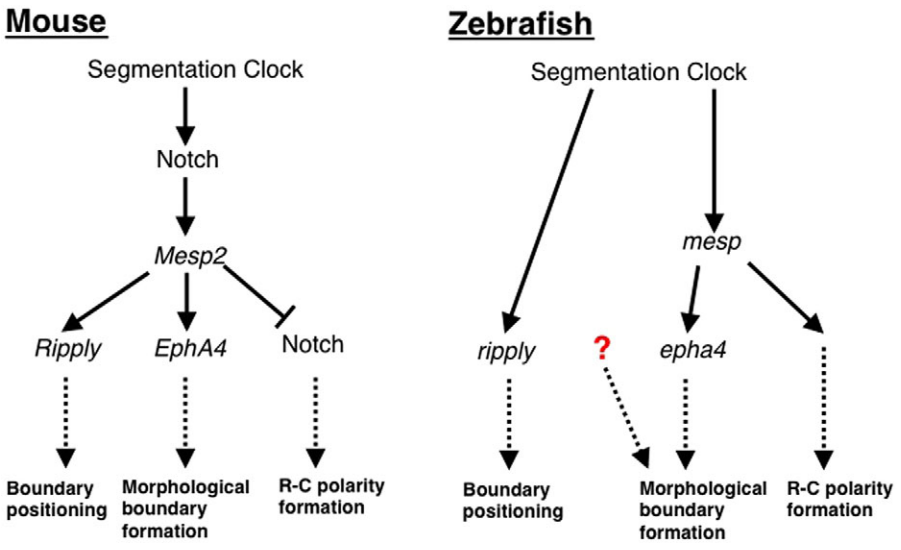

Fig. 8. Schematic representation showing the difference in the mechanism of somite segmentation between mouse and zebrafish. Model for the molecular network connecting the segmentation clock to somite formation in mouse (left) and zebrafish (right). In mouse, the functions of Notch signaling and Mesp2 connect the segmentation clock to the three different processes of somitogenesis (boundary positioning, morphological boundary formation and R-C polarity formation). However, in zebrafish, the segmentation clock regulates the expression of Ripply, in a manner that is independent of the function of Mesp, to determine the position of the somite boundary, and the function of Mesp is restricted to the generation of the morphological boundary and R-C polarity formation.

Development (2016) 143, 2842-2852 doi:10.1242/dev.133173

of National Institutes of Natural Sciences, with approval of the Institutional Animal Care and Use Committee (IACAC) of the National Institutes of Natural Sciences.

In situ hybridization

In situ hybridization was performed as described previously (Jowett and Yan, 1996). For synthesis of the mRNA probes, we amplified the fragments of *cxcl12a*, *smyhc*, *s100t* and *pax7* using the primers described in Table S3. These fragments were then cloned into the pBS-SK+ vector to use as a template for the RNA probe synthesis.

RNA and DNA injection

Capped mRNA, synthesized by use of a message mega-machine kit (Ambion) and plasmid or BAC DNA, purified using PureLink Midiprep Kit (Invitrogen), were dissolved in 0.2 M KCl with 0.05% Phenol Red and injected into one-cell stage zebrafish eggs using an IM300 microinjector (Narishige).

Transplantation analysis

The transplantation experiment was performed as described previously (Kawamura et al., 2005). Cells isolated from host embryos that had been injected with 1% Rhodamine-dextran (Molecular Probes) and 1% biotin-dextran were transferred to the margin of Mesp quadruple mutant embryos at the blastula stage. The host cells were identified by using Rhodamine Red X-NeutraAvidin (Molecular Probes).

Whole-mount immunostaining

For immunostaining, zebrafish embryos were fixed with 4% PFA/PBS at 4°C overnight.

After dechorionation, embryos were dehydrated by immersion in methanol at −20°C for more than 30 min. They were then hydrated by incubation in PBS containing 0.1% Triton X-100, 2% BSA and 1% DMSO for 1 h at room temperature. Then, embryos were incubated overnight at 4°C with primary antibody diluted 1:1000, 1:10, 1:2000 and 1:1000 for Tbx6 (Wanglar et al., 2014), 4D9 (DSHB), GFP (ThermoFisher, G10362) and Prox1 (AngiBio, 11-002P), respectively. After washing three times with PBS containing 0.1% Triton X-100 and 1% DMSO, the embryos were incubated with Alexa Fluor 488- or 555-conjugated secondary antibodies diluted 1:800. GFP signal was amplified using the TSA Plus fluorescence system (PerkinElmer). Double staining for Fn1 (1:100; Sigma, F3648) and Phalloidin (1:100; Molecular Probes) was performed without DMSO.

Mutagenesis using TALEN

The TALEN to target each gene was designed using TAL Effector Nucleotide Targeter 2.0 (https://tale-nt.cac.cornell.edu/node/add/talen-old; Table S1), assembled by using a modified Golden Gate Assembly Kit (Sakuma et al., 2013), and cloned into the pCS2+TAL3LL, pCS2+TAL3DD or pCS2+TAL3RR (Dahlem et al., 2012). One nanogram of each capped synthesized mRNA was injected into one-cell stage eggs of TL2. The mutation efficiency was assessed by performing a T7 endonuclease assay (Chen et al., 2012). The primers used to amplify the DNA fragment around the target site are described in Table S2. To obtain *mespaa; mespba* or *mespab; mespbb* double-mutant heterozygous fish, we performed sequential mutagenesis. First, *mespba* or *mespab* heterozygous F1 mutant fish were established by injection of TALEN mRNA and screening by direct sequencing of the mutated site in the F1 fish. Then, we injected TALEN into the eggs obtained by crossing F1 heterozygous fish and wild-type TL2 fish. The mosaic F2 fish were crossed to TL2 fish to obtain double heterozygous F3 fish, which were crossed to the wild-type fish to confirm that the two mutations were located in the same allele of the chromosome.

Generation of transgenic fish

Transgenic fish were generated and genotyped using standard techniques using primers as detailed in the supplementary Materials and Methods.

Acknowledgements

We thank Dr Koichi Kawakami, for providing materials and NIBB Core Research Facilities for their technical support, as well as all members of S.T.'s lab for their helpful discussions.

Competing interests

The authors declare no competing or financial interests.

Author contributions

T.Yab. and S.T. designed and conducted all the experiments and wrote the manuscript. T.Yam. and K.H. generated and provided materials for TALEN assembly.

Funding

This work was supported by grants from the Japan Society for the Promotion of Science [JSPS KAKENHI grant number 23657153 to S.T. and 24770218 to T.Yab.].

Supplementary information

Supplementary information available online at
http://dev.biologists.org/lookup/doi/10.1242/dev.133173.supplemental

References

Barresi, M. J., Stickney, H. L. and Devoto, S. H. (2000). The zebrafish slow-muscle-omitted gene product is required for Hedgehog signal transduction and the development of slow muscle identity. *Development* **127**, 2189-2199.

Barrios, A., Poole, R. J., Durbin, L., Brennan, C., Holder, N. and Wilson, S. W. (2003). Eph/Ephrin signaling regulates the mesenchymal-to-epithelial transition of the paraxial mesoderm during somite morphogenesis. *Curr. Biol.* **13**, 1571-1582.

Chen, J., Zhang, X., Wang, T., Li, Z., Guan, G. and Hong, Y. (2012). Efficient detection, quantification and enrichment of subtle allelic alterations. *DNA Res.* **19**, 423-433.

Chong, S.-W., Nguyet, L.-M., Jiang, Y.-J. and Korzh, V. (2007). The chemokine Sdf-1 and its receptor Cxcr4 are required for formation of muscle in zebrafish. *BMC Dev. Biol.* **7**, 54.

Cooke, J. and Zeeman, E. C. (1976). A clock and wavefront model for control of the number of repeated structures during animal morphogenesis. *J. Theor. Biol.* **58**, 455-476.

Cortés, F., Daggett, D., Bryson-Richardson, R. J., Neyt, C., Maule, J., Gautier, P., Hollway, G. E., Keenan, D. and Currie, P. D. (2003). Cadherin-mediated differential cell adhesion controls slow muscle cell migration in the developing zebrafish myotome. *Dev. Cell* **5**, 865-876.

Cutty, S. J., Fior, R., Henriques, P. M., Saúde, L. and Wardle, F. C. (2012). Identification and expression analysis of two novel members of the Mesp family in zebrafish. *Int. J. Dev. Biol.* **56**, 285-294.

Dahlem, T. J., Hoshijima, K., Jurynec, M. J., Gunther, D., Starker, C. G., Locke, A. S., Weis, A. M., Voytas, D. F. and Grunwald, D. J. (2012). Simple methods for generating and detecting locus-specific mutations induced with TALENs in the zebrafish genome. *PLoS Genet.* **8**, e1002861.

Dahmann, C., Oates, A. C. and Brand, M. (2011). Boundary formation and maintenance in tissue development. *Nat. Rev. Genet.* **12**, 43-55.

David, N. B., Sapède, D., Saint-Etienne, L., Thisse, C., Thisse, B., Dambly-Chaudière, C., Rosa, F. M. and Ghysen, A. (2002). Molecular basis of cell migration in the fish lateral line: role of the chemokine receptor CXCR4 and of its ligand, SDF1. *Proc. Natl. Acad. Sci. USA* **99**, 16297-16302.

Devoto, S. H., Melançon, E., Eisen, J. S. and Westerfield, M. (1996). Identification of separate slow and fast muscle precursor cells in vivo, prior to somite formation. *Development* **122**, 3371-3380.

Durbin, L., Sordino, P., Barrios, A., Gering, M., Thisse, C., Thisse, B., Brennan, C., Green, A., Wilson, S. and Holder, N. (2000). Anteroposterior patterning is required within segments for somite boundary formation in developing zebrafish. *Development* **127**, 1703-1713.

Felsenfeld, A. L., Curry, M. and Kimmel, C. B. (1991). The fub-1 mutation blocks initial myofibril formation in zebrafish muscle pioneer cells. *Dev. Biol.* **148**, 23-30.

Fleming, A., Keynes, R. and Tannahill, D. (2004). A central role for the notochord in vertebral patterning. *Development* **131**, 873-880.

Griffin, K. J. P. and Kimelman, D. (2002). One-Eyed Pinhead and Spadetail are essential for heart and somite formation. *Nat. Cell Biol.* **4**, 821-825.

Halpern, M. E., Ho, R. K., Walker, C. and Kimmel, C. B. (1993). Induction of muscle pioneers and floor plate is distinguished by the zebrafish no tail mutation. *Cell* **75**, 99-111.

Hart, D. O., Raha, T., Lawson, N. D. and Green, M. R. (2007). Initiation of zebrafish haematopoiesis by the TATA-box-binding protein-related factor Trf3. *Nature* **450**, 1082-1085.

Hubaud, A. and Pourquié, O. (2014). Signalling dynamics in vertebrate segmentation. *Nat. Rev. Mol. Cell Biol.* **15**, 709-721.

Jowett, T. and Yan, Y.-L. (1996). Double fluorescent in situ hybridization to zebrafish embryos. *Trends Genet.* **12**, 387-389.

Jülich, D., Geisler, R., Holley, S. A. and Consortium, T. S. (2005). Integrinalpha5 and delta/notch signaling have complementary spatiotemporal requirements during zebrafish somitogenesis. *Dev. Cell* **8**, 575-586.

Jülich, D., Cobb, G., Melo, A. M., McMillen, P., Lawton, A. K., Mochrie, S. G., Rhoades, E. and Holley, S. A. (2015). Cross-scale integrin regulation organizes ECM and tissue topology. *Dev. Cell* **34**, 33-44.

Development (2016) 143, 2842-2852 doi:10.1242/dev.133173

Kawamura, A., Koshida, S., Hijikata, H., Ohbayashi, A., Kondoh, H. and Takada, S. (2005). Groucho-associated transcriptional repressor ripply1 is required for proper transition from the presomitic mesoderm to somites. *Dev. Cell* **9**, 735-744.

Kimmel, C. B., Ballard, W. W., Kimmel, S. R., Ullmann, B. and Schilling, T. F. (1995). Stages of embryonic development of the zebrafish. *Dev. Dyn.* **203**, 253-310.

Kishimoto, Y., Koshida, S., Furutani-Seiki, M. and Kondoh, H. (2004). Zebrafish maternal-effect mutations causing cytokinesis defect without affecting mitosis or equatorial vasa deposition. *Mech. Dev.* **121**, 79-89.

Kitajima, S., Takagi, A., Inoue, T. and Saga, Y. (2000). MesP1 and MesP2 are essential for the development of cardiac mesoderm. *Development* **127**, 3215-3226.

Koshida, S., Kishimoto, Y., Ustumi, H., Shimizu, T., Furutani-Seiki, M., Kondoh, H. and Takada, S. (2005). Integrinalpha5-dependent fibronectin accumulation for maintenance of somite boundaries in zebrafish embryos. *Dev. Cell* **8**, 587-598.

Krol, A. J., Roellig, D., Dequéant, M.-L., Tassy, O., Glynn, E., Hattem, G., Mushegian, A., Oates, A. C. and Pourquié, O. (2011). Evolutionary plasticity of segmentation clock networks. *Development* **138**, 2783-2792.

Morimoto, M., Takahashi, Y., Endo, M. and Saga, Y. (2005). The Mesp2 transcription factor establishes segmental borders by suppressing Notch activity. *Nature* **435**, 354-359.

Morimoto, M., Sasaki, N., Oginuma, M., Kiso, M., Igarashi, K., Aizaki, K.-i., Kanno, J. and Saga, Y. (2007). The negative regulation of Mesp2 by mouse Ripply2 is required to establish the rostro-caudal patterning within a somite. *Development* **134**, 1561-1569.

Nakajima, Y., Morimoto, M., Takahashi, Y., Koseki, H. and Saga, Y. (2006). Identification of Epha4 enhancer required for segmental expression and the regulation by Mesp2. *Development* **133**, 2517-2525.

Nguyen-Chi, M. E., Bryson-Richardson, R., Sonntag, C., Hall, T. E., Gibson, A., Sztal, T., Chua, W., Schilling, T. F. and Currie, P. D. (2012). Morphogenesis and cell fate determination within the adaxial cell equivalence group of the zebrafish myotome. *PLoS Genet.* **8**, e1003014.

Nomura-Kitabayashi, A., Takahashi, Y., Kitajima, S., Inoue, T., Takeda, H. and Saga, Y. (2002). Hypomorphic Mesp allele distinguishes establishment of rostrocaudal polarity and segment border formation in somitogenesis. *Development* **129**, 2473-2481.

Oates, A. C., Morelli, L. G. and Ares, S. (2012). Patterning embryos with oscillations: structure, function and dynamics of the vertebrate segmentation clock. *Development* **139**, 625-639.

Oginuma, M., Niwa, Y., Chapman, D. L. and Saga, Y. (2008). Mesp2 and Tbx6 cooperatively create periodic patterns coupled with the clock machinery during mouse somitogenesis. *Development* **135**, 2555-2562.

Özbudak, E. M. and Lewis, J. (2008). Notch signalling synchronizes the zebrafish segmentation clock but is not needed to create somite boundaries. *PLoS Genet.* **4**, e15.

Rhee, J., Takahashi, Y., Saga, Y., Wilson-Rawls, J. and Rawls, A. (2003). The protocadherin papc is involved in the organization of the epithelium along the segmental border during mouse somitogenesis. *Dev. Biol.* **254**, 248-261.

Roy, S., Wolff, C. and Ingham, P. W. (2001). The u-boot mutation identifies a Hedgehog-regulated myogenic switch for fiber-type diversification in the zebrafish embryo. *Genes Dev.* **15**, 1563-1576.

Saga, Y. (2012a). The mechanism of somite formation in mice. *Curr. Opin. Genet. Dev.* **22**, 331-338.

Saga, Y. (2012b). The synchrony and cyclicity of developmental events. *Cold Spring Harb. Perspect. Biol.* **4**, a008201.

Saga, Y., Hata, N., Koseki, H. and Taketo, M. M. (1997). Mesp2: a novel mouse gene expressed in the presegmented mesoderm and essential for segmentation initiation. *Genes Dev.* **11**, 1827-1839.

Saga, Y., Miyagawa-Tomita, S., Takagi, A., Kitajima, S., Miyazaki, J. and Inoue, T. (1999). MesP1 is expressed in the heart precursor cells and required for the formation of a single heart tube. *Development* **126**, 3437-3447.

Sakuma, T., Hosoi, S., Woltjen, K., Suzuki, K., Kashiwagi, K., Wada, H., Ochiai, H., Miyamoto, T., Kawai, N., Sasakura, Y., et al. (2013). Efficient TALEN construction and evaluation methods for human cell and animal applications. *Genes Cells* **18**, 315-326.

Sasaki, N., Kiso, M., Kitagawa, M. and Saga, Y. (2011). The repression of Notch signaling occurs via the destabilization of mastermind-like 1 by Mesp2 and is essential for somitogenesis. *Development* **138**, 55-64.

Sawada, A., Fritz, A., Jiang, Y. J., Yamamoto, A., Yamasu, K., Kuroiwa, A., Saga, Y. and Takeda, H. (2000). Zebrafish Mesp family genes, mesp-a and mesp-b are segmentally expressed in the presomitic mesoderm, and Mesp-b confers the anterior identity to the developing somites. *Development* **127**, 1691-1702.

Schröter, C., Ares, S., Morelli, L. G., Isakova, A., Hens, K., Soroldoni, D., Gajewski, M., Jülicher, F., Maerkl, S. J., Deplancke, B. et al. (2012). Topology and dynamics of the zebrafish segmentation clock core circuit. *PLoS Biol.* **10**, e1001364.

Svetic, V., Hollway, G. E., Elworthy, S., Chipperfield, T. R., Davison, C., Adams, R. J., Eisen, J. S., Ingham, P. W., Currie, P. D. and Kelsh, R. N. (2007). Sdf1a patterns zebrafish melanophores and links the somite and melanophore pattern defects in choker mutants. *Development* **134**, 1011-1022.

Takahashi, Y., Koizumi, K., Takagi, A., Kitajima, S., Inoue, T., Koseki, H. and Saga, Y. (2000). Mesp2 initiates somite segmentation through the Notch signalling pathway. *Nat. Genet.* **25**, 390-396.

Takahashi, J., Ohbayashi, A., Oginuma, M., Saito, D., Mochizuki, A., Saga, Y. and Takada, S. (2010). Analysis of Ripply1/2-deficient mouse embryos reveals a mechanism underlying the rostro-caudal patterning within a somite. *Dev. Biol.* **342**, 134-145.

Trofka, A., Schwendinger-Schreck, J., Brend, T., Pontius, W., Emonet, T. and Holley, S. A. (2012). The Her7 node modulates the network topology of the zebrafish segmentation clock via sequestration of the Hes6 hub. *Development* **139**, 940-947.

Wanglar, C., Takahashi, J., Yabe, T. and Takada, S. (2014). Tbx protein level critical for clock-mediated somite positioning is regulated through interaction between Tbx and Ripply. *PLoS ONE* **9**, e107928.

Watanabe, T., Sato, Y., Saito, D., Tadokoro, R. and Takahashi, Y. (2009). EphrinB2 coordinates the formation of a morphological boundary and cell epithelialization during somite segmentation. *Proc. Natl. Acad. Sci. USA* **106**, 7467-7472.

Windner, S. E., Doris, R. A., Ferguson, C. M., Nelson, A. C., Valentin, G., Tan, H., Oates, A. C., Wardle, F. C. and Devoto, S. H. (2015). Tbx6, Mesp-b and Ripply1 regulate the onset of skeletal myogenesis in zebrafish. *Development* **142**, 1159-1168.

Yasuhiko, Y., Haraguchi, S., Kitajima, S., Takahashi, Y., Kanno, J. and Saga, Y. (2006). Tbx6-mediated Notch signaling controls somite-specific Mesp2 expression. *Proc. Natl. Acad. Sci. USA* **103**, 3651-3656.

Zhao, W., Ajima, R., Ninomiya, Y. and Saga, Y. (2015). Segmental border is defined by Ripply2-mediated Tbx6 repression independent of Mesp2. *Dev. Biol.* **400**, 105-117.

Supplementary Materials and Methods

Generation of transgenic fish

To generate *uas:mespba* fish, we amplified the full-length *mespba* fragment by PCR using ggaattcGACATGCAAACCTCAAGCAAG and ggctcgagTCATCTCCAGTAAGTCTGAGG, and cloned it into the EcoRI and XhoI site of pT2AUASMCS (a gift from Dr. Koichi Kawakami). For the generation of *tbx6:ggff* driver fish, pBS-hygroR-tol2R and pBS-tol2L-ampR cassettes were generated. The fragments of ampR and hygroR genes were amplified by PCR using GGAATTCTAGGGATAACAGGGTAATAACTTGGTCTGACAGTTACC, GGCTCGAGCACTTTTCGGGGAAATGTGC, GGAATTCTTGACAATTAATCATCGGCATAGTATATCGGCATAGTATAATACG ACTCACTATAGGAGGGCCATCATGAAAAAGCCTGAACTCAC and CTCGAGTAGGGATAACAGGGTAATCTATTCCTTTGCCCTCGGAC, and cloned into the EcoRI/XhoI and KpnI/ApaI sites of pBS-SK+ vector, respectively (pBS-ampR and pBS-hygroR). The *tol2L* and *tol2R* fragments were cut out from pT2AUASMCS and cloned into the NotI and EcoRI/KpnI site of pBS-ampR and pBS-hygroR, respectively. The homology arms were attached, flanking the ends of *hygroR-tol2R* and tol2L-ampR, by PCR using following primers; for *hygroR-tol2R* cassette, CCTCTGTGTGAAATGTGTCTGCAGTAGAACTCCAGTCGTTCTTGACAATTAA TCATCGGCATAGT and GTGAGCTGGGTCTTACTTCTCTGCTTGGCTGTTTTATTTTATCTGGCCTGTGT TTCAGACAC and for *tol2L-ampR* cassette,

TTAAAAGTCTTTTCCCACTTGCCCCTTAGTTTGATTTCCAGGATCCAGATCGA TCTGCGAAG and CTCAGTGTATAAGTCAGTGCCGTACGGATCGGTGGACGACCACTTTTCGGG GAAATGTGCG. The purified DNA fragments were introduced into the sw102 strain containing BAC (CH211-136M16) to introduce the *hygroR-tol2R* and *tol2L-ampR* cassettes into sites 14.5kbp upstream and 9.2kbp down stream of the Tbx transcription initiation site, respectively, by homologous recombination. Then the *ggff-pA-kanR* fragment was amplified by PCR using TTTAATATTCGATAAAGACAAACGTGAAGAAAGAGCAGACCCGGTCGCCAC CATGGTGAG and CTCTGTAATAGCAGTCGCTCAATCTCTGAGGTCCCAGAGCTGCGTGATCTGA TCCTTCAACTC. The fragment of *ggff-pA-kan* was introduced into the *tbx6* transcriptional initiation site of BAC (CH211-136M16) containing hygroR-tol2R and tol2L-ampR. The pT2A-hsf-ggff (a gift from Dr. Kawakami) was used as a template. Twenty-five picrograms of plasmid or BAC DNA was injected into the 1-cell- stage eggs of TL2 along with 50 pg of synthesized Tol2 transposase mRNA to obtain the transgenic fish. We used the following respective primers to check the genotypes of these transgenic fish; for *uas-mespba*, AGCGGAGACTCTAGAGGGTA and GGTTCTTCAGCCTCAATCTC and for *tbx6-ggff*, GTCTGAAGAACAACTGGGAG and TTCCGATGATGATGTCGCAC.

Genotyping of mutant and transgenic fish

To genotype the mutant generated by TALEN, we amplified the fragments of DNA

around the mutation site by PCR with primers used for the T7 endonuclease assay. To distinguish wild-type and mutant allele, we digested DNA fragments with BspHI, Hinp1I, PstI, HindIII, BccI, and HaeIII, for *mespba*^{kt1004}, *mespbb*^{kt1006}, *mespab*^{kt1002}, *mespab*^{kt1030}, *ripply1*^{kt1032} and *ripply2*^{kt1034}, respectively. Genotypes of *mespbb*^{kt1009} and *mespab*^{kt1017} were assessed by direct sequencing of PCR products. For genotyping *tbx6;ggff* and *uas;mespba*, the transgenes were detected by PCR by using the following primers: ; GTCTGAAGAACAACTGGGAG and TTCCGATGATGATGTCGCAC for *tbx6;ggff* and AGCGGAGACTCTAGAGGGTA and GGTTCTTCAGCCTCAATCTC for *uas;mespba*.

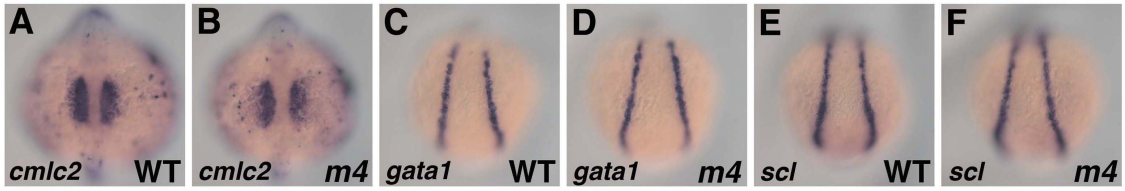

Fig. S1 Normal development of cardiac mesoderm and haematopoietic cells in the *mesp* quadruple mutant.

(A, B) Expression of *cmlc2* was not affected by mutations of the 4 mesp genes (100%; n=15). Embryos were fixed at the 17-somite stage. (C, D) Expression of *gata1* was not affected by mutations of the 4 *mesp* genes (100%; n=17). Embryos were fixed at the 11-somite stage. (E, F) Expression of *scl* was not affected by mutations of the 4 *mesp* genes (100%; n=15). Embryos were fixed at the11-somite stage.

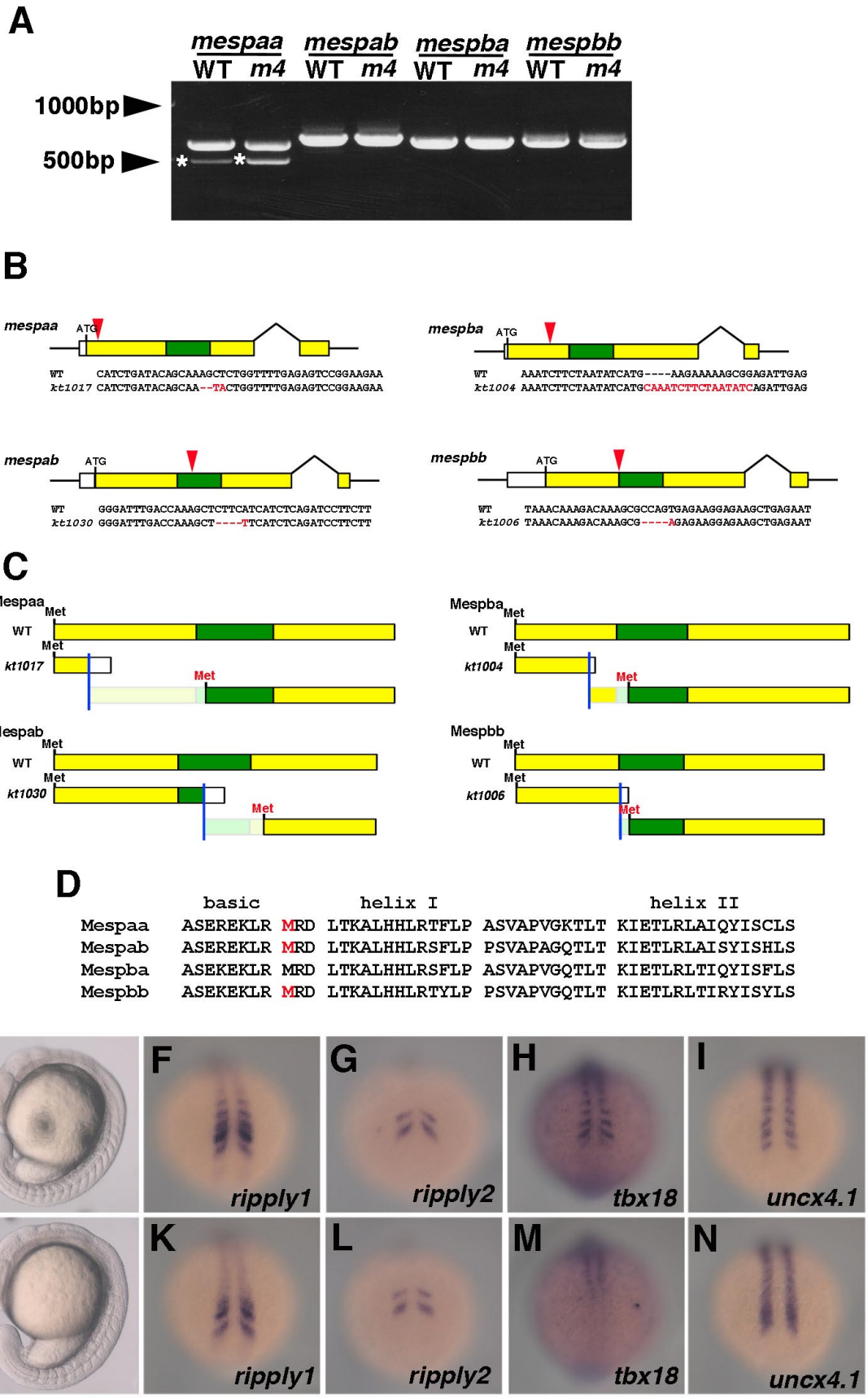

Fig. S2 Complete lack of Mesp function in the *mesp* quadruple mutant

(A) RT-PCR products of *mesp* genes from the wild type and the *mesp* quadruple mutant embryo. Electrophoresis of *mesps* cDNA amplified by RT-PCR. The total RNA was isolated from wild type or *mesp* quadruple mutant embryos at the 8-somite stage. After reaction with reverse transcriptase, cDNA fragment containing the whole sequence of the coding region of th 4 *mesps* was amplified by PCR. All fragments were confirmed by direct sequencing and any unexpected splicing variant was not detected. Asterisks indicate non-specifically amplified PCR products, checked by direct sequencing.

(B-F) Generation of *mespab*^{kt1030} *and mespbb*^{kt1006} allele.

(B) Schematic diagrams showing mutations generated in the 4 *mesp* genes. Colored boxes indicate the coding regions; especially, green boxes show the basic helix-loop-helix domain. Red arrowheads indicate the approximate position of each mutation. Sequences around the mutation sites are also shown. Red characters in these sequences indicate mutated sequence. (C) Schematic diagrams of predicted protein structures produced from *mesp* mutant alleles shown in (B). Colored boxes indicate regions where amino acids in the same frame as the original could be translated and green boxes indicate the basic helix-loop-helix domain. White boxes indicate regions where different frames could be translated by frame-shift mutations. Blue lines indicate positions of the mutations. Possible coding frames containing the basic helix-loop-helix domain are also displayed. “Met” colored with red indicate presumptive positions of the translational initiation site. (D) Amino acids sequences of the basic helix-loop-helix domain of the 4 Mesp proteins. Red-colored M correspond to the red-colored Met shown in (C). Note that the presumptive translation products from mutant alleles of

mespaa, *mespab*, and *maspbb* could not contain the whole basic helix-loop-helix domain. (E,-N) Wild type (E, F, G,H,I) and another *mesp* quadruple mutant carrying distinct alleles from those mainly examined in this study (J,K,L,M,N). At the 16-somite stage, the morphology of *mespaa*$^{kt1017/kt1017}$; *mespba*$^{kt1004/kt1004}$; *mespab*$^{kt1030/kt1030}$; *mespbb*$^{kt1006/kt1006}$ was obviously identical to that of *mespaa*$^{kt1017/kt1017}$; *mespba*$^{kt1004/kt1004}$; *mespab*$^{kt1002/kt1002}$; *mespbb*$^{kt1009/kt1009}$, which were mainly examined in this study (E,F; See Figure 2). The expression *ripply1*, *ripply2*, *tbx18* and *uncx4.1* of *mespaa*$^{kt1017/kt1017}$; *mespba*$^{kt1004/kt1004}$; *mespab*$^{kt1030/kt1030}$; *mespbb*$^{kt1006/kt1006}$ was also identical those of *mespaa*$^{kt1017/kt1017}$; *mespba*$^{kt1004/kt1004}$; *mespab*$^{kt1002/kt1002}$; *mespbb*$^{kt1009/kt1009}$ at the 11-somite stage (F-I, K-N; See Figure 3 and 5)

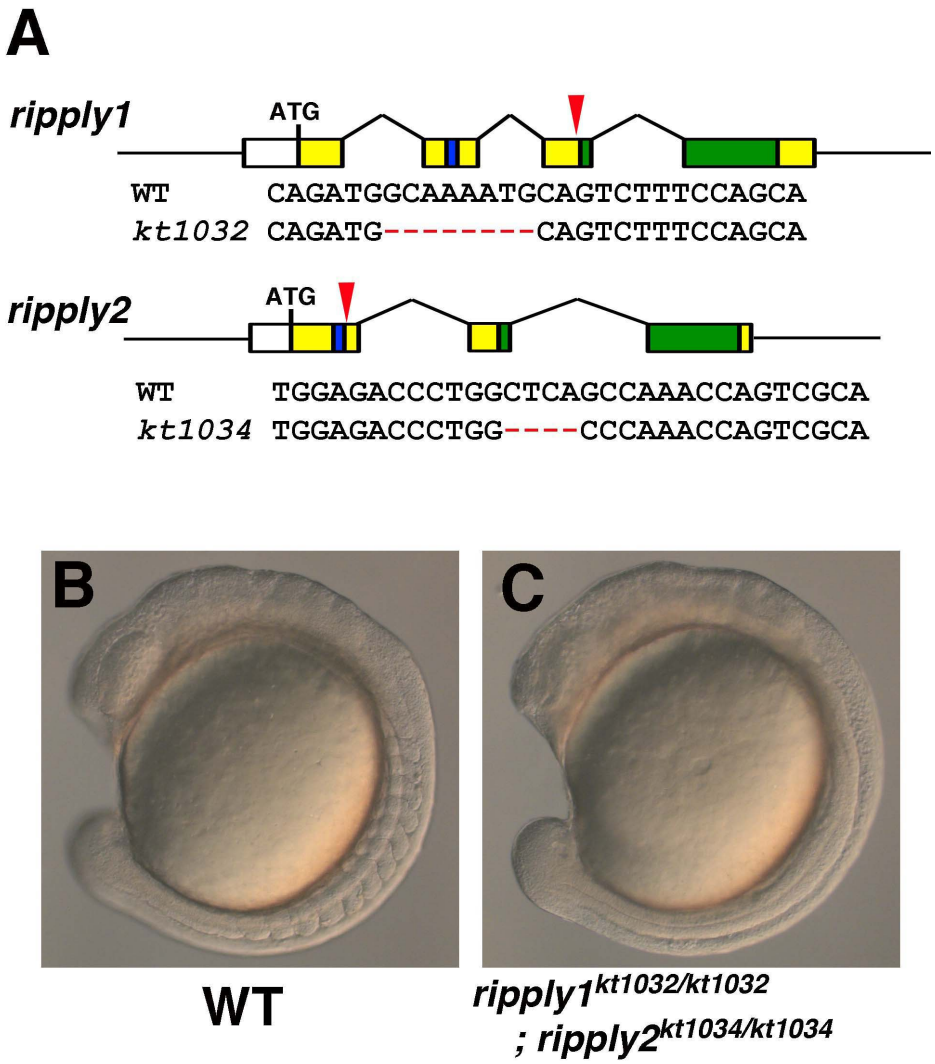

Fig. S3 Generation of *ripply1* and *ripply2* double mutant using TALENs

(A) Schematic diagram showing mutations of *ripply1* and *ripply2*. Colored boxes indicate the coding regions of Ripply1 and Ripply2 proteins; green boxes indicate the Ripply-homology domain, which is required for physical interaction with Tbx6, and blue boxes indicate the WRPW motif, which is essential for the interaction with Groucho. Red arrowheads indicate approximate positions of the mutations. The DNA sequences around the mutation sites are given below the schematic diagrams. Red bars indicate the mutated sequence. (B, C) The morphologies of *rippley1;ripply2* double mutant embryo at the 13-somites stage.

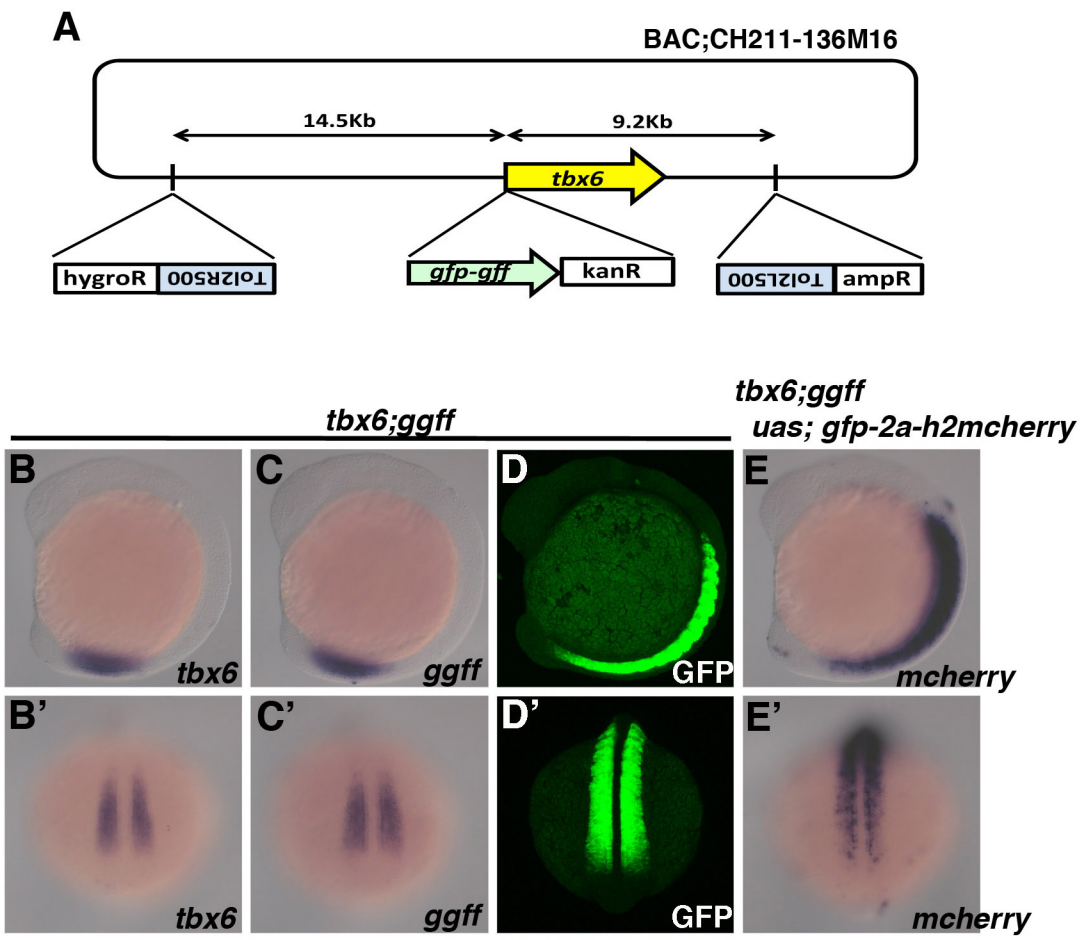

Fig. S4 Generation of *tbx6:ggff* transgenic fish

(A) Schematic diagram showing construction of the transgene. *tol2* and *ggff-pA-kan* cassette were introduced into CH211-136M16 by using homologous recombination in E.coli. (B,C) The expression pattern of *ggff* mRNA was almost identical to that of endogenous *tbx6* mRNA at the 11-somite stage. (D) The expression of GFP-GFF fusion protein (GGFF) was assessed by immunostaining using anti-GFP antibody. The expression GGFF was detected in the anterior PSM and mature somite region at the 11-somite stage. (E) *mcherry* expression in tbx6:ggff/uas:gfp-2a-h2a-mcherry double transgenic embryo at the 11-somite stage. Lateral and dorsal views of embryos are shown in B-E and B'-E', respectively.

Table S1. The list of the module of TALEN used for mutagenesis

	pCS2+TAL3-DD	pCS2+TAL3-RR
***mespaa*^{kt1017}**	HD NG NG HD HD NN NN NI HD NG HD NG HD NI NI	NI NI HD HD NI NN HD NI NG HD NG NN NI NG NI HD
***mespba*^{kt1004}**	NI NN NG HD NI NI NI NG HD NG NG HD NG NI NI NG NI	HD NG NG HD NI NN HD HD NG HD NI NI NG HD NG HD HD
***mespab*^{kt1002}**	HD HD NI NG HD NN NI NG NG HD HD NN NN NI NG NN HD NG NG NG	HD HD NI NN NG NG NN NG HD NG NG HD HD NI NN HD
***mespab*^{kt1030}**	HD HD NN NI NI NG NN NI NN NN NN NI NG NG NG NN NI HD HD	NN NN NI NN NN NG NI NI NN NI NI NN NN NI NG HD NG NN NI
***mespbb*^{kt1006}** ***mespbb*^{kt1009}**	HD HD NG NI NN NG NI NI NI HD NI NI NI NN NI HD NI	HD HD HD NG HD NI NG NG HD NG HD NI NN HD NG NG HD NG HD HD
***ripply1*^{kt1032}**	NN HD HD HD NN NN NG NI NI HD NI HD NG NI HD NI NI HD	NN NI HD NI NN NN NN NG NN HD NG NN NN NI NI NI NN NI HD
***ripply2*^{kt1034}**	HD NG NN NI NI NI NG NN NN NI HD NN HD NN NI NI NG HD NI	NN HD NN NI HD NG NN NN NG NG NG NN NN HD NG NN NI NN HD

Table S2. The list of the primers used for T7-endonuclease assay

	Forward primer	Reverse primer
***mespaa*^{kt1017}**	GCCTCCACGTTTTCTCTTCAGC	cCAGGAAACTTCGATTTGGGAC
***mespba*^{kt1004}**	AACCGATGGAGCAGTTCCAG	GTTTGTCCTACCGGAGCTAC
***mespab*^{kt1002}**	GACCATGGAGTTTAACCTTCCTCC	GGAGTTTCTCTCGTTCGCTTGCTG
***mespab*^{kt1030}**	GCTGGAAGACAACTGGAAGG	TGTAGCTAATGGCAAGACGG
***mespbb*^{kt1006}** ***mespbb*^{kt1009}**	ACTCCTGGAGCTCAGACTCC	GGTAGGTACGTCCTGAGGTG
***ripply1*^{kt1032}**	CATAAACACCGGACAGGAAGC	CAAACCAATTGCTCAAGCCAGAG
***ripply2*^{kt1034}**	CTCTTTCCACGGACACTATGG	GAAGATGGAGAGCTTGTGCTG

Table S3. The list of the primers used for cDNA cloning for mRNA probe synthesis.

	Forward primer	Reverse primer
cxcl12[7]	ggaattcTGATCGTAGTAGTCGCTCTG	ggctcgagTAACACGACAAACACGGAGC
smyhc	ggaattcACAACACACAGGACAACCC	ggctcgagCGAATCGGGAGGAGTTGTCA
s100t	ggaattcAACTCCGAGAATGCCTCCAC	cccggtaccGGGTTTGCGCCTCATGGAAC
pax7	ggaattcAGGAACAGTTCCTCGAATG	ggctcgagATGTCAGGGTAGTGTGTC